Marine Pollution Bulletin 150 (2020) 110736

Contents lists available at ScienceDirect

Marine Pollution Bulletin

journal homepage: www.elsevier.com/locate/marpolbul

Baseline

Health risk assessment of polycyclic aromatic hydrocarbons in coastal soils of Koh Samed Island (Thailand) after the oil spill incident in 2013

Ronbanchob Apiratikul[a], Siwatt Pongpiachan[b,*], Muhammad Zaffar Hashmi[c]

[a] Department of Environmental Science, Suan Sunandha Rajabhat University, Bangkok, Thailand
[b] School of Social & Environmental Development, National Institute of Development Administration (NIDA), Bangkok, Thailand
[c] Department of Chemistry, COMSATS University, Park Road, Chak Shahzad, Islamabad 44000, Pakistan

ARTICLE INFO

Keywords:
PAHs
Human health risk assessment
Koh Samed Island
Oil spill

ABSTRACT

Health risks of human exposures to 12 Polycyclic aromatic hydrocarbons (PAHs) in coastal soils of Koh Samed Island (KSI), Thailand, were evaluated after the coastal areas were cleaned up of the 2013 oil-spill contamination. The risk assessment quantified both total cancer and non-cancer risks for four groups of receptors using average PAHs concentrations. Two exposure pathways (incidental ingestion and dermal contact) were selected to evaluate the risks, and three methods were used to calculate the total cancer risks to determine an appropriate assessment method. The non-cancer risk was represented by the total Hazard Index (HI). The contributions of each PAH to the total cancer risk and total HI were also investigated. The total cancer risk (3.53×10^{-10} to 9.12×10^{-8}) and total HI ($4.35\times10^{-6\ \text{to}\ 2.13\times10^{-3}}$) from this work were relatively lower than the USEPA baselines (10^{-6} for the cancer risk and 1 for the HI) and were quite low when compared with other works in the literature. Benzo(a)pyrene made the highest contribution to the total cancer risk (61.82%), while benzo[g,h,i]perylene made the highest contribution to the total HI (62.41%). In regard to the contributions of the two exposure routes, dermal contact contributed the most to the total cancer risk, while incidental ingestion contributed the most to the total HI.

Polycyclic aromatic hydrocarbons (PAHs) are toxic organic compounds that are commonly found in the environment. These chemicals are harmful to both humans and wildlife and can cause both cancer and non-cancer related adverse health effects. PAHs can be found in all compartments of the environment (e.g. aerosols, terrestrial soils, marine deposits, and agricultural products) and typically persist for long periods of time because of the complexity of their chemical structures which makes them very difficult to degrade; thus, many PAHs have a tendency to accumulate in living and non-living things (Pongpiachan, 2015; Pongpiachan et al., 2017a; Pongpiachan et al., 2017b; Pongpiachan et al., 2018). Furthermore, they also undergo long-range transportation (Tamamura et al., 2007; Yang et al., 2007). One important source of PAHs is oil spills, and PAHs were found to represent 3.9% by weight of the oil spill from the Macondo well during the Deepwater Horizon oil spill incident (Allan et al., 2012). In 2013, Thailand confronted a massive oil spill in the Gulf of Thailand caused by a ruptured pipeline that was owned by PTT Global Chemical Public Company Limited (PTTGC); the pipeline burst when oil was being transferred from an undersea well to a tanker on July 27th. Approximately 50,000 L (310 bbl) of crude oil were spilled, and this oil heavily contaminated the northern parts of the Gulf of Thailand, an area which included Koh Samed Island (KSI), one of the most popular tourist attractions in the region. The incident had adverse impacts on the economy particularly in regards to both tourism and fisheries, and it also undermined the confidence of investors. Even though the contaminated sites have been cleaned up by the removal of the crude oil, there are still some remaining questions about the levels of remnant PAHs and their potential effects on health. In previous work, Pongpiachan et al. (Pongpiachan et al., 2018) characterised the PAH contamination in the coastal soils of KSI about 2 years after the incident and classified the PAH emission sources by using statistical applications. The study results indicated that the average concentration of PAHs was much lower than the values specified in international guidelines and no significant differences were observed in all of the PAH congeners collected from seven different location groups. In addition, the majority of PAHs in KSI coastal soils were found to have been appreciably influenced by the oil spill accident. Importantly, the PAHs with a high molecular weight (especially PAHs with 5 to 6 rings) were found to be the dominant species present in KSI's coastal soils, and this has led to serious concerns with respect to adverse health effects

* Corresponding author.
E-mail addresses: Ronbanchob.Ap@ssru.ac.th (R. Apiratikul), pongpiajun@gmail.com (S. Pongpiachan).

https://doi.org/10.1016/j.marpolbul.2019.110736
Received 7 September 2019; Received in revised form 12 November 2019; Accepted 14 November 2019
Available online 21 November 2019
0025-326X/

through long-term bioaccumulation and biomagnification of these PAHs. Thus, further study of the health risks associated with these PAHs is necessary.

The aims of the present work were as follows: i) to evaluate the environmental health risks of human exposures to the PAHs in coastal soils of KSI in terms of both the total cancer and non-cancer risks, and 12 dominant PAHs were selected to calculated the risks by using various methods; ii) to compare the cancer risk calculation methods; iii) to compare the effect of receptor grouping on the risks; iv) to investigate the contribution of each PAH and each exposure pathway to the risks; and v) to compare the risks associated with the PAHs from KSI with those of other sites as reported in the literature.

Twelve probably carcinogenic PAH compounds, namely, phenanthrene (Phe), anthracene (An), fluoranthene (Fluo), pyrene (Pyr), benzo(a)anthracene (B[*a*]A), chrysene (Chry), benzo(b)fluoranthene (B[*b*]F), benzo(k)fluoranthene (B[*k*]F), benzo(a)pyrene (B[*a*]P), dibenz(a,h)anthracene (D[*a*,*h*]A), indeno[1,2,3-c,d]pyrene (Ind), and benzo[*g*,*h*,*i*]perylene (B[*g*,*h*,*i*]P), were analysed to determine the concentrations in coastal soils from 69 sampling sites around Koh Samed Island (KSI) as described in the previous study (Pongpiachan et al., 2018). Averages and standard deviation (SD) values for individual PAH concentrations and the total 12 PAH concentrations from all of the sampling sites were calculated and used to represent the overall PAH contamination at KSI because the PAH concentrations are comparatively homogeneously distributed around the island's coast according to the previous study (Pongpiachan et al., 2018). The average concentration of PAHs was further used in the risk calculations that will be described shortly.

The standard models of lifetime cancer risk recommended by the U.S. Environmental Protection Agency (US-EPA, 1991) were applied in this study to assess the cancer risks of PAHs in KSI's coastal soils. Incidental ingestion of and dermal contact with PAH contaminated soils were assumed to be the two main exposure routes responsible for the adverse health effects as the cancer risks from the inhalation route were relatively low and seemed to be insignificant when compared to the ingestion and dermal contact risks (Chen et al., 2018). The chronic daily intake due to ingestion and the chronic daily intake for dermal exposures were calculated by Eqs. (1) and (2), respectively:

$$CDI_i = \frac{CS \times IR \times EF \times ED \times CF}{BW \times AT_c} \quad (1)$$

$$CDI_d = \frac{CS \times SA \times AF \times DAF \times EF \times ED \times CF}{BW \times AT_c} \quad (2)$$

The terms in Eqs. (1) and (2) can be defined as follows: CDI_i = chronic daily intake due to ingestion (mg $_{PAH}$ $kg_{body\ weight}^{-1}$ day^{-1}), CDI_d = chronic daily intake for dermal exposure (mg_{PAH} $kg_{body\ weight}^{-1}$ day^{-1}, CS = concentration of PAH in soil (ng_{PAH} g_{soil}^{-1}), IR = ingestion rate (assumed to be 50 mg_{soil} day^{-1}), SA = skin surface area (4700 cm^2 available for contact), AF = skin adherence factor (0.3 mg_{soil} cm^{-2} day^{-1}), DAF = dermal absorption factor of 0.03 (represents 3% of adsorbed soil to skin from the total skin adhered soil), EF = exposure frequency (40 day $year^{-1}$), ED = exposure duration (10 years), CF = conversion factor (10^{-6} mg_{PAH} ng_{PAH}^{-1} × 10^{-3} g_{soil} mg_{soil}^{-1} = 10^{-9} mg_{PAH} g_{soil} ng_{PAH}^{-1} mg_{soil}^{-1}), BW = body weight (53 kg-body weight), AT_c = averaging time for cancer risk (25550 days). The values of these parameters were recommended by the Agency for Toxic Substances and Disease Registry (ATSDR, 2005) for a general group of receptors (without division by the receptor's age interval, i.e. childhood, adolescence, and adulthood).

The cancer risks of each PAH compound can be calculated by Eqs. (3) to (5):

$$CR_i = SF_i \times CDI_i \quad (3)$$

$$CR_d = SF_d \times CDI_d \quad (4)$$

$$TCR = CR_i + CR_d \quad (5)$$

where the terms in the cancer risk equations can be defined as follows: CR_i = cancer risk due to ingestion (unitless), CR_d = cancer risk due to dermal contact (unitless), SF_i = cancer slope factor for ingestion (mg_{PAH}^{-1} $kg_{body\ weight}$ day), SF_d = dermal cancer slope factor (mg_{PAH}^{-1} $kg_{body\ weight}$ day), TCR = total cancer risk (unitless).

Some researchers have proposed the use of a modified model in which a body weight correction factor is added (Peng et al., 2011); this changes Eqs. (3) and (4) into Eqs. (6) and (7):

$$CR_i = SF_i \times \sqrt[3]{\frac{BW}{70}} \times CDI_i \quad (6)$$

$$CR_d = SF_d \times \sqrt[3]{\frac{BW}{70}} \times CDI_d \quad (7)$$

In this study, the assessment of cancer risks was then performed by using three methods, which are described below in detail.

Method A, the concentrations of each individual PAH compound were directly used as the CS in Eqs. (1) and (2) without converting to B[*a*]P toxic equivalent concentrations. The chronic daily intakes were consequently used to calculate the cancer risks by Eqs. (3) to (5). The cancer slope factor of 1.5 mg_{PAH}^{-1} kg $_{body\ weight}$ day was arbitrarily used for both exposure pathways as SF_i and SF_d in Eqs. (3) and (4). The value of the slope factor was also applied for all of the PAH compounds (Pongpiachan et al., 2017a; Sun et al., 2016).

Method B, the concentrations of each individual PAH compound were converted to B[*a*]P toxic equivalent concentrations by multiplying its toxic equivalent factor (TEF) before the calculations of the cancer risks. B[*a*]P is widely recognised as a representative of carcinogenic PAH compounds, and cancer slope factors (SF_i and SF_d) are available for B[*a*]P. The TEFs as introduced by Hester et al. (Hester et al., 1998) were used in this study, and the values are listed in the TEF column of Table 2. The B[*a*]P toxic equivalent concentrations of each individual PAH compound were further used as CS in Eqs. (1) and (2) to calculate the chronic daily intakes. The cancer risks due to ingestion (CR_i) and dermal contact (CR_i) were then calculated by using Eqs. (3) to (5) with an SF_i of 7.3 mg_{PAH}^{-1} kg $_{body\ weight}$ day (US-EPA, 1993) and SF_d of 25 mg_{PAH}^{-1} kg $_{body\ weight}$ day (Knafla et al., 2006), respectively.

Method C, the concentrations of each individual PAH compound were first converted to B[*a*]P toxic equivalent concentrations and were then substituted as CS in Eqs. (1) and (2) to calculate the chronic daily intakes. Subsequently, the cancer risks due to ingestion (CR_i) and dermal contact (CR_i) were calculated by using a body weight correction factor with Eqs. (6), (7), and (5) and with an SF_i of 7.3 mg_{PAH}^{-1} kg $_{body\ weight}$ day (US-EPA, 1993) and SF_d of 25 mg_{PAH}^{-1} kg $_{body\ weight}$ day (Knafla et al., 2006), respectively.

Assessments of non-cancer risks, incidental ingestion and dermal contact of PAH contaminated soils were also assumed to be the major pathways for non-cancer health effects. The average daily dose of chemical intake due to incidental ingestion and dermal contact were determined by using the generic equations proposed by the USEPA (US-EPA, 1991) as shown in Eqs. (8) and (9):

$$ADD_i = \frac{CS \times IR \times EF \times ED \times CF}{BW \times AT_{nc}} \quad (8)$$

$$ADD_d = \frac{CS \times SA \times AF \times DAF \times EF \times ED \times CF}{BW \times AT_{nc}} \quad (9)$$

The terms in Eqs. (8) and (9) can be defined as follows: ADD_i = average daily dose due to ingestion (mg $_{PAH}$ kg $_{body\ weight}^{-1}$ day^{-1}), ADD_d = average daily dose for dermal exposure (mg_{PAH} $kg_{body\ weight}^{-1}$ day^{-1}), AT_{nc} = averaging time for non-cancer risk (3650 days). The other terms have the same meanings and values as given for Eqs. (1) and (2).

Non-cancer risks of each PAH compound can be evaluated by using Eqs. (10) to (12):

$$HQ_i = ADD_i / RfD_i \quad (10)$$

$$HQ_d = ADD_d/RfD_d \quad (11)$$

$$HI = HQ_i + HQ_d \quad (12)$$

The terms in Eqs. (10) to (12) can be defined as follows: HQ_i = hazard quotient due to ingestion (unitless), HQ_d = hazard quotient due to dermal contact (unitless), RfD_i = reference dose for ingestion (mg_{PAH} kg $_{body\ weight}^{-1}$ day^{-1}), RfD_d = reference dose (mg_{PAH}^{-1} kg $_{body\ weight}$ day), HI = hazard index (unitless).

The reference dose (RfD) can be searched from EPA-IRIS database (US-EPA, 2019). The RfD_i values for PAH compounds that were listed in the database are as follows: 0.3 mg kg^{-1} day^{-1} for anthracene; 0.04 mg kg^{-1} day^{-1} for fluorene and fluoranthene; 0.03 mg kg^{-1} day^{-1} for pyrene; and 3.07×10^{-4} mg kg^{-1} day^{-1} for benzo(a)pyrene. Due to the lack of information for the RfD_i and RfD_d of the other PAH compounds, both the RfD_i and RfD_d were assumed to have the value of benzo(a)pyrene (3.07×10^{-4} mg kg^{-1} day^{-1}) for these other PAH compounds in this study. This value was selected because it is the lowest known value among the RfDs of the PAH compounds shown above and would yield the highest HI possible for a stringent non-cancer risk evaluation.

The results for the cancer risks derived with method A are summarised in Table 1. The average of the total cancer risk from all of the PAHs was found to be 1.33×10^{-9}. The USEPA has set a baseline for the Superfund program in which a potential cancer risk assessment is deemed necessary when values are $> 10^{-4}$. Such values might lead to adverse effects on human health and warrant risk management actions, e.g. site remediation; thus, risks should be seriously evaluated and the remediation goal must reduce the risks to $< 10^{-6}$ (US-EPA, 1989; US-EPA, 2001). With method A, the risk was relatively low as the value was 750 times lower than the value of the USEPA baseline for determining remediation goals (10^{-6}). The upper bound for the population scale of the average total cancer risk ($\mu_{upper\ bound}$) was estimated by using the Student's *t*-statistic for the confidential interval of 99.9% ($\alpha = 0.001$) via the following equation:

$$\mu_{upper\ bound} = \bar{x} + \frac{t_{\alpha/2,n-1}SD}{\sqrt{n}} \quad (13)$$

where $\bar{x} = 1.33 \times 10^{-9}$, $n = 69$, $t_{0.0005,\ 68} = 3.44$, and SD (standard deviation) $= 2.53 \times 10^{-9}$. This resulted in a $\mu_{upper\ bound}$ of 2.38×10^{-9}, which is still 420 times lower than the value for USEPA baseline's remediation goal of 10^{-6}. These results can be attributed to the fact that the magnitude of total cancer risks of KSI fell in the 'acceptable level' range, and the findings indicate that the region does not pose serious cancer risks.

With method A, B[*g,h,i*]P had the highest percentage contribution of 62.41% to the total cancer risks for overall PAHs. This was because the major factor that affects the total cancer risk for method A is only the original PAH concentration and individual toxicity considerations are not taken into account. Since B[*g,h,i*]P had the highest average concentration in KSI's coastal soil among the 12 PAHs, it had the highest cancer risks for all pathways and for the total cancer risk in this method. However, it is not quite reasonable to use the model in method A for evaluating the contributions of individual PAHs to the cancer risks because the toxicity of each PAH varies and this was not considered in the cancer risk assessment model despite the fact that toxicity depends heavily on the individual PAH's structure.

The concentrations of 12 probably carcinogenic PAH compounds in the form of B[*a*]P toxic equivalents were computed by using toxic equivalent factors, and these results are summarised in Table 2 under the headings of CS in B[*a*]P equivalents. These B[*a*]P toxic equivalent concentrations were then used for an assessment of the cancer risks of individual PAH compounds according to Eqs. (1) to (5) for method B, and these results are also displayed in Table 2.

In this second method (method B), the averages of total cancer risks for individual probably carcinogenic PAHS in KSI ranged from 0.69×10^{-13} for An to 0.72×10^{-9} for B[*a*]P, and the total cancer risk from all PAHs was 1.17×10^{-9}. The observed sequence in decreasing order of percentage contribution of each PAH congener to the total cancer risk of all PAHs was B[a]P (61.82%) > B[*b*]F (17.20%) > B[*g,h,i*]P (14.63%) > B[*k*]F (5.01%) > Chry (0.50%) > Fluo (0.48%) > D[*a,h*]A (0.18%) > B[*a*]A (0.12%) > Ind (0.04%) > Pyr (0.02%) > Phe (0.014%) > An (0.006%). Thus, it can be concluded that B[*a*]P had the highest contribution to the total cancer risk in this work. It is interesting to note that the top three individual PAHs contributing to the total cancer risk (B[*a*]P, B[*b*]F, and B[*g,h,i*]P) had contributions that summed to 93.65% for the total cancer risk from all PAHs. These top three PAHs were congeners of high molecular weight PAHs (HMW) with 5–6 rings, and these congeners accounted for 92% of the total PAH concentrations in KSI in the previous work (Pongpiachan et al., 2018). Thus, it seems that the HMW PAHs are the main culprits responsible for the total cancer risks. However, the major factors that affect the total cancer risk in this method are the original PAH concentration and its toxic equivalent factor to B[*a*]P, and HMWs tend to have high toxic equivalent factors. Hence, the high concentrations of PAH in the coastal soil and high toxic equivalent factors were the main factors driving the high contribution to the overall total cancer risk of B[*a*]P, B[*b*]F, and B[*g,h,i*]P.

The contribution of exposure routes was also investigated. Dermal contact had a percentage contribution of 74.34% in regard to the total cancer risk, while incidental ingestion had a contribution of approximately 25.66%. This implies that dermal contact is the major pathway for cancer risks from PAH exposures into the human body in the study area.

The average of total cancer risks from 69 samples derived with

Table 1
Statistical descriptions of the PAH cancer risks (method A) in coastal areas of KSI.

PAHs at KSI (n = 69)		CS Avg ± SD	CR_i Avg ± SD	CR_d Avg ± SD	Total cancer risk Avg ± SD	Contribution of each PAH
		(ng g^{-1})	(−)	(−)	(−)	(%)
1	Phe	0.784 ± 1.40	$(1.74 \pm 3.09) \times 10^{-11}$	$(1.47 \pm 2.62) \times 10^{-11}$	$(3.21 \pm 5.71) \times 10^{-11}$	2.41
2	An	0.330 ± 0.879	$(0.73 \pm 1.95) \times 10^{-11}$	$(0.62 \pm 1.65) \times 10^{-11}$	$(1.35 \pm 3.60) \times 10^{-11}$	1.01
3	Fluo	0.264 ± 0.536	$(0.59 \pm 1.19) \times 10^{-11}$	$(0.50 \pm 1.01) \times 10^{-11}$	$(1.08 \pm 2.19) \times 10^{-11}$	0.81
4	Pyr	0.473 ± 0.741	$(1.05 \pm 1.64) \times 10^{-11}$	$(0.89 \pm 1.39) \times 10^{-11}$	$(1.94 \pm 3.03) \times 10^{-11}$	1.45
5	B[*a*]A	0.639 ± 1.91	$(1.42 \pm 4.22) \times 10^{-11}$	$(1.20 \pm 3.57) \times 10^{-11}$	$(2.62 \pm 7.80) \times 10^{-11}$	1.96
6	Chry	0.459 ± 1.47	$(1.02 \pm 3.26) \times 10^{-11}$	$(0.86 \pm 2.76) \times 10^{-11}$	$(1.88 \pm 6.03) \times 10^{-11}$	1.41
7	B[*b*]F	4.78 ± 10.6	$(1.06 \pm 2.36) \times 10^{-10}$	$(0.90 \pm 2.00) \times 10^{-10}$	$(1.95 \pm 4.35) \times 10^{-10}$	14.67
8	B[*k*]F	2.78 ± 6.70	$(6.16 \pm 14.84) \times 10^{-11}$	$(0.52 \pm 1.26) \times 10^{-10}$	$(1.14 \pm 2.74) \times 10^{-10}$	8.54
9	B[*a*]P	1.72 ± 4.38	$(3.81 \pm 9.71) \times 10^{-11}$	$(3.22 \pm 8.21) \times 10^{-11}$	$(0.70 \pm 1.79) \times 10^{-10}$	5.27
10	Ind	0.0110 ± 0.0836	$(0.24 \pm 1.85) \times 10^{-12}$	$(0.21 \pm 1.57) \times 10^{-12}$	$(0.45 \pm 3.42) \times 10^{-12}$	0.03
11	D[*a,h*]A	0.00449 ± 0.0373	$(0.99 \pm 8.27) \times 10^{-13}$	$(0.84 \pm 7.00) \times 10^{-13}$	$(0.18 \pm 1.53) \times 10^{-12}$	0.01
12	B[*g,h,i*]P	20.3 ± 60.2	$(0.45 \pm 1.33) \times 10^{-9}$	$(0.38 \pm 1.13) \times 10^{-9}$	$(0.83 \pm 2.46) \times 10^{-9}$	62.41
Total 12 PAHs		32.6 ± 61.8	$(0.72 \pm 1.37) \times 10^{-9}$	$(0.61 \pm 1.16) \times 10^{-9}$	$(1.33 \pm 2.53) \times 10^{-9}$	100

Table 2
Statistical descriptions of B[*a*]P equivalent concentrations and PAH cancer risks (method B) in coastal areas of KSI.

PAHs at KSI (n = 69)		TEF	CS in B[*a*]P equivalents Avg ± SD	CR_i Avg ± SD	CR_d Avg ± SD	Total cancer risk Avg ± SD	Contribution of each PAH
			(ng g^{-1})	(−)	(−)	(−)	(%)
1	Phe	0.0005	0.000392 ± 0.000698	(4.23 ± 7.53) × 10^{-14}	(1.22 ± 2.18) × 10^{-13}	(1.65 ± 2.93) × 10^{-13}	0.014
2	An	0.0005	0.000165 ± 0.000440	(1.78 ± 4.74) × 10^{-14}	(0.52 ± 1.37) × 10^{-13}	(0.69 ± 1.85) × 10^{-13}	0.006
3	Fluo	0.05	0.0132 ± 0.0268	(1.42 ± 2.89) × 10^{-12}	(4.13 ± 8.38) × 10^{-12}	(0.56 ± 1.13) × 10^{-11}	0.48
4	Pyr	0.001	0.000473 ± 0.000741	(5.10 ± 7.99) × 10^{-14}	(1.48 ± 2.32) × 10^{-13}	(1.99 ± 3.11) × 10^{-13}	0.02
5	B[*a*]A	0.005	0.00320 ± 0.00953	(0.34 ± 1.03) × 10^{-12}	(1.00 ± 2.98) × 10^{-12}	(1.34 ± 4.01) × 10^{-12}	0.12
6	Chry	0.03	0.0138 ± 0.0442	(1.49 ± 4.77) × 10^{-12}	(0.43 ± 1.38) × 10^{-11}	(0.58 ± 1.86) × 10^{-11}	0.50
7	B[*b*]F	0.1	0.478 ± 1.065	(0.52 ± 1.15) × 10^{-10}	(1.49 ± 3.33) × 10^{-10}	(2.01 ± 4.47) × 10^{-10}	17.20
8	B[*k*]F	0.05	0.139 ± 0.335	(1.50 ± 3.61) × 10^{-11}	(0.43 ± 1.05) × 10^{-10}	(0.58 ± 1.41) × 10^{-10}	5.01
9	B[*a*]P	1	1.72 ± 4.38	(1.85 ± 4.73) × 10^{-10}	(0.54 ± 1.37) × 10^{-9}	(0.72 ± 1.84) × 10^{-9}	61.82
10	Ind	0.1	0.00110 ± 0.00836	(1.19 ± 9.02) × 10^{-13}	(0.34 ± 2.61) × 10^{-12}	(0.46 ± 3.51) × 10^{-12}	0.04
11	D[*a*,*h*]A	1.1	0.00494 ± 0.0411	(0.53 ± 4.43) × 10^{-12}	(0.15 ± 1.28) × 10^{-11}	(0.21 ± 1.73) × 10^{-11}	0.18
12	B[*g*,*h*,*i*]P	0.02	0.407 ± 1.20	(0.44 ± 1.30) × 10^{-10}	(1.27 ± 3.76) × 10^{-10}	(1.71 ± 5.06) × 10^{-10}	14.63
Total 12 PAHs			2.78 ± 4.68	(3.00 ± 5.05) × 10^{-10}	(0.87 ± 1.46) × 10^{-9}	(1.17 ± 1.97) × 10^{-9}	100.00

method B was 1.17 × 10^{-9}. This value was still very low when compared to the remediation goals of the USEPA, i.e. it was 856 times lower than 10^{-6} baseline. The upper bound for the population value of the average total cancer risk ($\mu_{\text{upper bound}}$) was also calculated by using Eq. (13) with a confidential interval of 99.9% (α = 0.001), $\bar{x}$ = 1.17 × 10^{-9}, n = 69, $t_{0.0005,\ 68}$ = 3.44, and SD = 1.97 × 10^{-9}. This resulted in a $\mu_{\text{upper bound}}$ of 1.98 × 10^{-9}, which was still 506 times lower than the value of USEPA's baseline remediation goal of 10^{-6}. Thus, it can be concluded that even with this method, the total cancer risk of KSI contamination was found to be acceptable.

For the method C, the B[*a*]P toxic equivalent concentrations of each PAH compound from Table 2 were used for an assessment of the cancer risks according to Eqs. (1), (2), (6), (7), and (5), in which was a body weight correction factor was included in the evaluation of cancer risk. These results are displayed in Table 3.

The total cancer risk from all PAHs from this method was 1.06 × 10^{-9}, which was about 940 times lower than the value of 10^{-6} used for the USEPA's baseline remediation goal. The percentages of PAH compounds that contributed to the total cancer risk in this method were the same as those in the previous method (method B), which B[*a*]P shared the highest proportion while An had the lowest contribution. This was because the input concentrations of these two methods were the same, as were the B[*a*]P toxic equivalent concentrations. The upper bound for the population value of the average total cancer risk for this method (method C) was also calculated with a confidential interval of 99.9% (α = 0.001) by using Eq. (13) and the result was of 1.81 × 10^{-9}. This value was still 554 times lower than the value of USEPA's baseline remediation goal of 10^{-6}. Thus, it can be inferred again that the total cancer risk of KSI contamination was found to be acceptable with this method,

The averages of total cancer risk from all PAHs were 1.33 × 10^{-9}, 1.17 × 10^{-9}, and 1.06 × 10^{-9} for methods A, B, and C, respectively. These values had the same order magnitude. Statistical analyses at the significant level (α) of 0.001 were used in this study for a comparison of mean values between the population scales of all three methods. The methods were paired as three pairs (A vs B, B vs C, and C vs A) and the total cancer risk between each method was statistically tested by using *t*-tests. We found that there were no significant differences between the total cancer risks at the population scale for all pairs. This means that the body weight correction factor from the method C did not have much of an effect on the total cancer risk calculations in this study. Hence, method B was more reasonable for evaluating the contributions of individual PAHs to the total cancer risk than method A as the TEF was included in method B. Furthermore, method B was more comfortable for calculating the cancer risks than method C due to its simplicity.

The total cancer risks from this work were compared with those from the literature. The results from the three methods used for TCR evaluations for PAHs in this work were compared with those from other works in the literature. To facilitate the comparisons, only 12 PAHs from the other works were evaluated in computing the total cancer risk even though there were > 12 PAHs in the previous studies. The results were represented on a logarithmic scale and are shown in Fig. 1. The abbreviations in the figure showing the TCR for average PAH concentrations can be defined follows:

Table 3
Statistical descriptions of cancer risks (method C) in coastal areas of KSI[a].

PAHs at KSI (n = 69)		CR_i Avg ± SD	CR_d Avg ± SD	Total cancer risk Avg ± SD	Contribution of each PAH
		(−)	(−)	(−)	(%)
1	Phe	(3.85 ± 6.86) × 10^{-14}	(1.12 ± 1.99) × 10^{-13}	(1.50 ± 2.67) × 10^{-13}	0.014
2	An	(1.62 ± 4.32) × 10^{-14}	(0.47 ± 1.25) × 10^{-13}	(0.63 ± 1.68) × 10^{-13}	0.006
3	Fluo	(1.30 ± 2.64) × 10^{-12}	(3.76 ± 7.64) × 10^{-12}	(0.51 ± 1.03) × 10^{-11}	0.48
4	Pyr	(4.65 ± 7.28) × 10^{-14}	(1.35 ± 2.11) × 10^{-13}	(1.81 ± 2.84) × 10^{-13}	0.02
5	B[*a*]A	(3.14 ± 9.37) × 10^{-13}	(0.91 ± 2.71) × 10^{-12}	(1.22 ± 3.65) × 10^{-12}	0.12
6	Chry	(1.35 ± 4.34) × 10^{-12}	(0.39 ± 1.26) × 10^{-11}	(0.53 ± 1.69) × 10^{-11}	0.50
7	B[*b*]F	(0.47 ± 1.05) × 10^{-10}	(1.36 ± 3.03) × 10^{-10}	(1.83 ± 4.08) × 10^{-10}	17.20
8	B[*k*]F	(1.37 ± 3.29) × 10^{-11}	(3.96 ± 9.53) × 10^{-11}	(0.53 ± 1.28) × 10^{-10}	5.01
9	B[*a*]P	(1.69 ± 4.31) × 10^{-10}	(0.49 ± 1.25) × 10^{-9}	(0.66 ± 1.68) × 10^{-9}	61.82
10	Ind	(1.08 ± 8.22) × 10^{-13}	(0.31 ± 2.38) × 10^{-12}	(0.42 ± 3.20) × 10^{-12}	0.04
11	D[*a*,*h*]A	(0.49 ± 4.04) × 10^{-12}	(0.14 ± 1.17) × 10^{-11}	(0.19 ± 1.57) × 10^{-11}	0.18
12	B[*g*,*h*,*i*]P	(0.40 ± 1.18) × 10^{-10}	(1.16 ± 3.43) × 10^{-10}	(1.56 ± 4.61) × 10^{-10}	14.63
Total 12 PAHs		(2.73 ± 4.60) × 10^{-10}	(0.79 ± 1.33) × 10^{-9}	(1.06 ± 1.79) × 10^{-9}	100.00

[a] CS B[*a*]P equivalents are the same as those in Table 2.

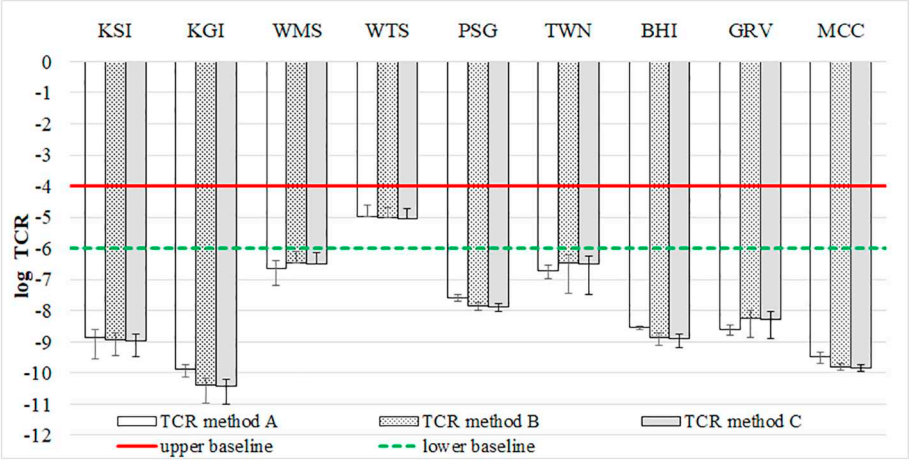

Fig. 1. Comparison of total cancer risks between this work (KSI) and other sites on a logarithmic scale.

KSI: Coastal soils and sediments of Koh Samui Island (this work)
KGI: Terrestrial soils of King George Island (Pongpiachan et al., 2017a)
WMS: Marine sediments from around the world collected by Pongpiachan et al. (Pongpiachan et al., 2017a)
WTS: Terrestrial soils from around the world collected by Pongpiachan et al. (Pongpiachan et al., 2017a)
PSG: Coastal sediments of the Persian Gulf, Iran (Aghadadashi et al., 2017)
TWN: Sediments in Kaohsiung Harbor, Taiwan (Chen & Chen, 2011)
BHI: Surface sediments in the Bohai Sea, China (Li et al., 2015)
GRV: Surface sediments in the Guan River Estuary, China (He et al., 2014)
MCC: Sediments in Mecoacán Lake, Mexico (Armenta-Arteaga & Elizalde-Gonzfilez, 2003)

Fig. 1 shows that the total cancer risks from all methods for all sites were below a lower baseline of 10^{-6} except for those at WTS, and all site results were lower than the upper baseline of 10^{-4} for all methods. These data indicate that the risks from all sites are acceptable, but the risks at WTS are quite high even though there is no need to urgently clean up the site.

All calculation results for the total cancer risk derived from each method (A, B, and C) at each site were then paired and used in *t*-tests for the statistical comparison between each pair (A vs. B, B vs. C, and A vs. C). The results for all sites showed that there was no difference between the values for method B and method C at the α of 0.001. Nevertheless, while there were no differences among all of the methods for some sites (i.e. KSI, WMS, WTS, TWN, and GRV), the method A results were slightly higher than those for method B and method C for some sites (KGI, PSG, BHI, and MCC).

Hence, it can be inferred from the findings in this section that the cancer risk assessment conducted with method B is reasonable for further use as a representative method for total cancer risk calculations in this study. Specifically, this method includes the TEFs of all PAH species (while method A does not) and it does not require complex calculations like those in method C; meanwhile, method B still produced results similar to those for the complex method C. However, method A can still be recommended for rough estimations of the overall total cancer risks from all PAHs without concern as to the contribution of each PAH to the cancer risks.

It can be seen from the Fig. 1 that the KGI location had the lowest cancer risk from PAHs as it is a pristine area and there is not much interference from human activities as it is located at around the Earth's South Pole quite far from any city while the WTS had the highest cancer risk. In addition, the total cancer risks of WTS are the only one that overcame the lower baseline. This indicating that all locations except the WTS did not show any significant cancer risks.

Method B was used to compute the total cancer risk and results were obtained for each receptor group, i.e. general, childhood, adolescence, and adulthood. Then, comparisons between each group were made. The values for the model parameters of the general group were the values that were applied in the previous sections, which were those recommended by ATSDR (ATSDR, 2005), while those of the other groups were the values as summarised by Chen et al. (Chen et al., 2018). The results are shown in Fig. 2.

According to the figure, the suggested ATSDR values for the parameters gave a significantly lower total cancer risk in the general group than the risks in the other receptor groups, for which we used the summarised values by Chen et al. (Chen et al., 2018) (for α of 0.001). The average total cancer risks for the childhood, adolescence, and adulthood groups were roughly 46, 25, and 34 times higher than that of the general group, respectively, for all sites.

The three receptor groups (childhood, adolescence, and adulthood) were also paired to check for differences in total cancer risk between each group by using *t*-tests. The results showed that there was no significant difference between the total cancer risk of these groups for each site. However, there was an exception detected at two sites in which the total cancer risk of the childhood group was significantly higher than those of the other receptor groups at these sites (PSG and MCC).

The total cancer risk of this work (KSI), which was obtained from the summarised values of parameters given by Chen et al. (Chen et al., 2018), was lower than the lower baseline of 10^{-6}, which indicates that the cancer risks from PAHs at Koh Samui Island in Rayong, Thailand, have been at a safe level since the 2013 oil spill incident was cleaned up. However, when considering the other sites with these values from Chen et al. (Chen et al., 2018), the average of the total cancer risk of the three groups was shifted to a relatively higher total cancer risk. This resulted in the exceedance of the lower baseline for some sites (WMS and TWN) and also an exceedance of the upper baseline for WTS. Meanwhile, the risk at the other sites was still less than the lower baseline.

The contribution of the exposure routes was also studied. Dermal contact had the largest contribution to the total cancer risk rather than incidental ingestion. The percentages of the distribution of the dermal contact contribution were 74.34, 55.49, 71.37, and 63.98 for the general, childhood, adolescence, and adulthood groups, respectively. Meanwhile, for incidental ingestion, the distribution percentages were 25.66, 44.51, 28.63, and 36.02 for the general, childhood, adolescence, and adulthood groups, respectively. These values were the same for all listed sites in Fig. 2. This reason for this was related to the fact that the contributions depended on the input parameters of the risk model for

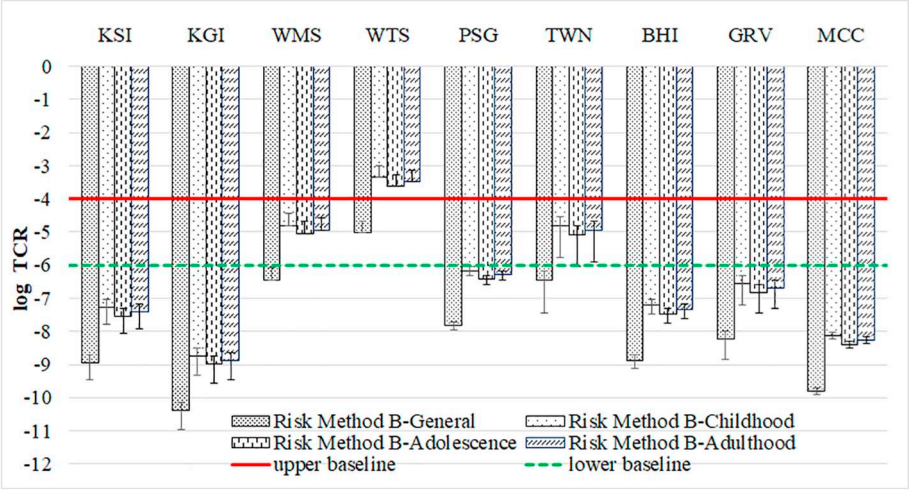

Fig. 2. The total cancer risks of each receptor group from various sites.

all sites and all groups of receptors.

The contributions of each PAH according to method B are summarised in Fig. 3. It was interesting to note that method B (for all groups of receptors) and method C gave the same pattern of PAH contributions to the total cancer risk. This was because both of these methods used toxic equivalent factors to convert PAH concentrations to B[*a*]P equivalent concentrations.

Fig. 3 shows that B[*a*]P made the main contribution to the total cancer risk for most sites. However, an exception was found at GRV in which D[*a*,*h*]A shared the highest percentage in terms of the contribution. These results were due to the high concentrations and high toxic equivalent factors of B[*a*]P and D[*a*,*h*]A at those sites. For this work (KSI), the contribution from Fluo was low (0.48%), and this PAH shared the lowest percentage of the contribution among all sites. In addition, low contribution percentages of Chry, D[*a*,*h*]A, and Ind were observed in this work (0.50%, 0.18%, and 0.04%, respectively), and the KSI values were lower than those of most sites. The lowest percentages of Chry (0.27%), D[*a*,*h*]A (0%), and Ind (0.02%) were found at GRV, MCC, and KGI, respectively. Meanwhile, B[*b*]F and B[*g*,*h*,*i*]P from this work shared high percentages in terms of the contribution (17.20% and 14.63%, respectively) when compared with those from the other sites in the figure.

The non-cancer risks of PAHs in this work (KSI) and the other works from the literature were calculated with the total Hazard Index (HI) according to Eqs. (8) to (12) for all 12 PAHs. The values of model parameters were applied for each group of receptors in the same manner as described above. The results are summarised in Table 4 and are also presented on a logarithmic scale of HI in Fig. 4.

The total HI of the general group in this work ranged from 4.35×10^{-6} to 3.62×10^{-5} with an average of 2.03×10^{-5}, which resulted in a negative value for the HI on a logarithmic scale. The total HI of PAHs from the other three receptor groups at KSI was higher than that from the general group. However, the logarithms of the total HI from all groups for KSI were still less than zero, which is equivalent to a total HI value that is less than one. This can interpreted as there being no substantial risks of non-carcinogenic impacts at KSI in Thailand. The contribution percentages of each PAH to the total HI from this work (KSI) are shown in Table 4 and patterns were the same as those in Table 1 where B[*g*,*h*,*i*]P shared the highest contribution to the total HI (62.41%). This was due to the fact that the total HI was calculated from the raw concentration of PAHs, which resulted in the same pattern of PAH distributions in regard to the total HI, concentrations, and also to the total cancer risk with method A. The average of the total HI value for the general group at each site was ranked from low to high as KGI < MCC < KSI < GRV < BHI < PSG < TWN < WMS < WTS. The average of the total HI value from this study (KSI) was the

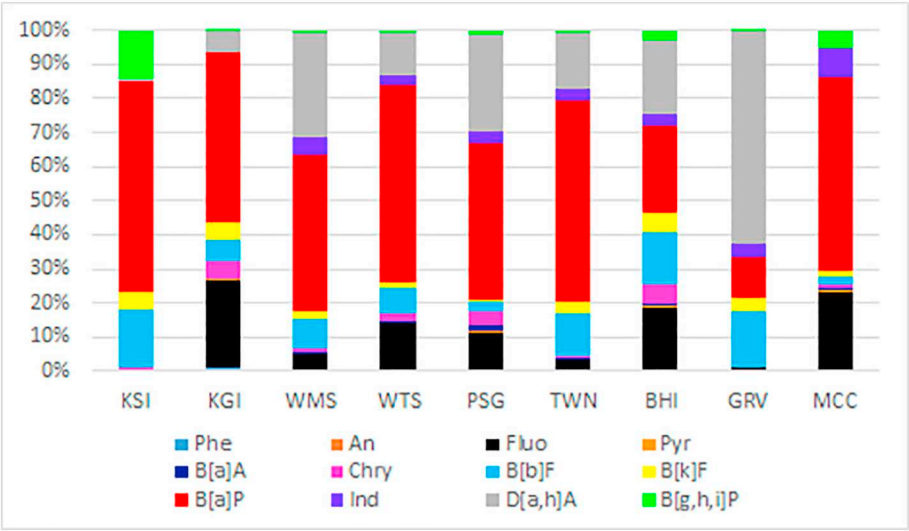

Fig. 3. Contribution of each PAH to the total cancer risk according to method B for each site.

Table 4
Statistical descriptions of HQs and HIs in coastal areas of KSI for the general group.

PAHs at KSI (n = 69)		HQ_i Avg ± SD	HQ_d Avg ± SD	HI Avg ± SD	Contribution of each PAH
		(−)	(−)	(−)	%
1	Phe	$(2.64 \pm 4.71) \times 10^{-7}$	$(2.24 \pm 3.98) \times 10^{-7}$	$(4.88 \pm 8.69) \times 10^{-7}$	2.41
2	An	$(1.11 \pm 2.96) \times 10^{-7}$	$(0.94 \pm 2.51) \times 10^{-7}$	$(2.05 \pm 5.47) \times 10^{-7}$	1.01
3	Fluo	$(0.89 \pm 1.81) \times 10^{-7}$	$(0.75 \pm 1.53) \times 10^{-7}$	$(1.64 \pm 3.34) \times 10^{-7}$	0.81
4	Pyr	$(1.60 \pm 2.50) \times 10^{-7}$	$(1.35 \pm 2.11) \times 10^{-7}$	$(2.95 \pm 4.61) \times 10^{-7}$	1.45
5	B[*a*]A	$(2.16 \pm 6.43) \times 10^{-7}$	$(1.82 \pm 5.44) \times 10^{-7}$	$(0.40 \pm 1.19) \times 10^{-6}$	1.96
6	Chry	$(1.55 \pm 4.97) \times 10^{-7}$	$(1.31 \pm 4.20) \times 10^{-7}$	$(2.86 \pm 9.17) \times 10^{-7}$	1.41
7	B[*b*]F	$(1.61 \pm 3.59) \times 10^{-6}$	$(1.36 \pm 3.04) \times 10^{-6}$	$(2.97 \pm 6.62) \times 10^{-6}$	14.67
8	B[*k*]F	$(0.94 \pm 2.26) \times 10^{-6}$	$(0.79 \pm 1.91) \times 10^{-6}$	$(1.73 \pm 4.17) \times 10^{-6}$	8.54
9	B[*a*]P	$(0.58 \pm 1.48) \times 10^{-6}$	$(0.49 \pm 1.25) \times 10^{-6}$	$(1.07 \pm 2.73) \times 10^{-6}$	5.27
10	Ind	$(0.37 \pm 2.82) \times 10^{-8}$	$(0.31 \pm 2.39) \times 10^{-8}$	$(0.69 \pm 5.21) \times 10^{-8}$	0.03
11	D[*a*,*h*]A	$(0.15 \pm 1.26) \times 10^{-8}$	$(0.13 \pm 1.06) \times 10^{-8}$	$(0.28 \pm 2.32) \times 10^{-8}$	0.01
12	B[*g*,*h*,*i*]P	$(0.69 \pm 2.03) \times 10^{-5}$	$(0.58 \pm 1.72) \times 10^{-5}$	$(1.27 \pm 3.75) \times 10^{-5}$	62.41
Total 12 PAHs		$(1.10 \pm 2.08) \times 10^{-5}$	$(0.93 \pm 1.76) \times 10^{-5}$	$(2.03 \pm 3.84) \times 10^{-5}$	100

third from the lowest, which was about 10 times higher than the lowest (KGI), about 49,325 times lower than the baseline of 1 (log HI = 0), and about 7904 times lower than the highest (WTS).

It is interesting to note that the average total HI of PAHs from the childhood, adolescence, and adulthood groups at all sites in Fig. 4 were about 59, 26, and 39 times higher than that from the general group, respectively. The *t*-test results were applied to check for the difference between the total HI from the general group and that from each specific receptor group. The results showed that the general group had a different total HI from those of the other specific receptor groups at the α of 0.001. This also reflects the fact that the summarised values by Chen et al. (Chen et al., 2018) gave significantly higher total HI values for the specific groups than the total HI for the general group in which the values of model parameters used were those recommended by ATSDR (ATSDR, 2005).

The *t*-tests were also applied to check for the difference between the total HI of each specific group of receptors. The results showed that there was no difference between the total HI from specific groups and those from the corresponding receptor groups for KSI (this work), WMS, WTS, and TWN. However, the total HI of the childhood group for KGI, PSG, GRV, and MCC was different from that of the adolescence group, and specifically, the HI of the childhood group was greater than that of the adolescence group. Meanwhile, the total HI values of the three specific groups of receptors for BHI were all different from each other and were ranked as $HI_{childhood} > HI_{adulthood} > HI_{adolescence}$.

As demonstrated in Fig. 4, all of the logarithms of total HI values observed at most sites were less than zero, which indicates that no adverse human health impacts should be caused by these PAHs. Nevertheless, the logarithms of total HI values of all three specific groups from WTS were above zero, thus suggesting a higher risk for non-carcinogenic impacts by PAHs for this site.

The contributions of the exposure pathways were also investigated. Incidental ingestion made the main contribution to the total HI and had distribution percentages of 54.17, 73.31, 57.87, and 65.85 for the general, childhood, adolescence, and adulthood groups, respectively. In comparison, dermal contact had a contribution distribution of about 45.83% for the general group, 26.69% for the childhood group, 42.13% for the adolescence group, and 34.15% for the adulthood group. This reason for this was also related to the fact that the contributions depended on the input parameters of the risk model for all sites and all groups of receptors.

The conclusions are followings. This work assessed the environmental risks of human exposures to 12 PAHs in coastal soils at Koh Samed Island (KSI), Thailand. All calculation methods showed that the total cancer risks in this work were significantly ($p < .001$) lower than the USEPA baseline for determining remediation goals (10^{-6}) for all groups of receptors. This indicates that the total cancer risks at KSI are now acceptable following the clean-up of the site of PAH contamination from a 2013 oil spill. We found that method B, which considers the toxic equivalence of all PAHs, was a suitable method to compute the total cancer risk and to evaluate the contribution percentages of each PAH to the total cancer risk. However, method A, which depends only

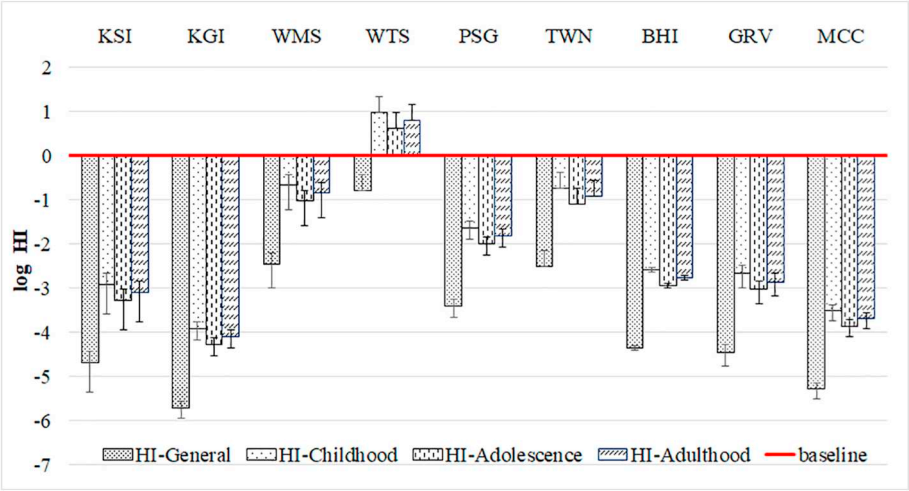

Fig. 4. The Hazard Index (HI) of each receptor group from various sites.

on the raw concentration of PAHs, may still be useful for obtaining rough estimates of the total cancer risk, but it is not suitable for evaluating the contribution percentages of each PAH to the total cancer risk. The total HI computed during the non-cancer risk assessment of this work was less than one, which indicates that adverse human health impacts from PAHs at KSI are unlikely. Nevertheless, it is interesting to remark that there are some limitations or considerations due to assumption in the calculation of the total cancer risk and total HI because these are assumed some determined values which could be different according to gender, body weight, and hours of exposure. The findings from this work could be used to help to inspire confidence in tourists and investors about the safety of the island following the clean-up of PAHs in coastal areas that were contaminated by the oil spill in 2013. In addition, the results from this work could be useful in the selection of an appropriate method for conducting risk assessments.

CRediT authorship contribution statement

Ronbanchob Apiratikul: Conceptualization, Methodology, Software, Validation, Formal analysis, Investigation, Data curation, Visualization, Writing - original draft, Writing - review & editing. **Siwatt Pongpiachan**: Conceptualization, Funding acquisition, Project administration, Investigation, Resources, Supervision, Validation. **Muhammad Zaffar Hashmi**: Validation.

Declaration of competing interest

The authors declare that they have no known competing financial interests or personal relationships that could have appeared to influence the work reported in this paper.

Acknowledgements

The authors acknowledge Ms. Mattanawadee Hattayanone, Ms. Chormsri Choochuay, and Ms. Woranut Deelaman for their contributions to the field and laboratory work. This study was financially supported by the Research Centre of the National Institute of Development Administration (RC-NIDA), Thailand.

References

Aghadadashi, V., Mehdinia, A., Molaei, S., 2017. Origin, toxicological and narcotic potential of sedimentary PAHs and remarkable even/odd n-alkane predominance in Bushehr Peninsula, the Persian Gulf. Mar. Pollut. Bull. 114 (1), 494–504.

Allan, S.E., Smith, B.W., Anderson, K.A., 2012. Impact of the Deepwater Horizon oil spill on bioavailable polycyclic aromatic hydrocarbons in Gulf of Mexico coastal waters. Environ. Sci. Technol. 46 (4), 2033–2039.

Armenta-Arteaga, G., Elizalde-Gonzfilez, M.E., 2003. Contamination by PAHs, PCBs, PCPs and heavy metals in the Mecoacfin Lake estuarine water and sediments after oil spilling. Journal of Soils & Sediments 3 (1), 35–40.

ATSDR, 2005. Health Consultation. Review of Sediment Data of Sylvester's (A/K/A) Gilson Road Site. U.S. Department of health and human services, Division of Health Assessment and Consultation, Atlanta, Georgia Retrieved from. http://www.atsdr.cdc.gov/HAC/pha/Gilson%20Road%20Site/GilsonRoadHCFinal.pdf.

Chen, C.-W., Chen, C.-F., 2011. Distribution, origin, and potential toxicological significance of polycyclic aromatic hydrocarbons (PAHs) in sediments of Kaohsiung Harbor, Taiwan. Mar. Pollut. Bull. 63 (5–12), 417–423.

Chen, Y., Zhang, J., Zhang, F., Liu, X., Zhou, M., 2018. Contamination and health risk assessment of PAHs in farmland soils of the Yinma River Basin, China. Ecotoxicol. Environ. Saf. 156, 383–390.

He, X., Pang, Y., Song, X., Chen, B., Feng, Z., Ma, Y., 2014. Distribution, sources and ecological risk assessment of PAHs in surface sediments from Guan River Estuary, China. Mar. Pollut. Bull. 80, 52–58.

Hester, R.E., Harrison, R.M., Larsen, J.C., Larsen, P.B., 1998. Chemical carcinogens. In: Harrison, R.E., Hester, R.E. (Eds.), Air Pollution and Health. Royal Society of Chemistry, pp. 33–56.

Knafla, A., Phillipps, K., Brecher, R., Petrovic, S., Richardson, M., 2006. Development of a dermal cancer slope factor for benzo[a]pyrene. Regul. Toxicol. Pharmacol. 45, 59–168.

Li, S., Zhang, S., Dong, H., Zhao, Q., Cao, C., 2015. Presence of aliphatic and polycyclic aromatic hydrocarbons in near-surface sediments of an oil spill area in Bohai Sea. Mar. Pollut. Bull. 100, 169–175.

Peng, C., Chen, X., Liao, M., Wang, Z., Ouyang, W., Jiao, B.Y., 2011. Polycyclic aromatic hydrocarbons in urban soils of Beijing: status, sources, distribution and potential risk. Environ. Pollut. 159 (3), 802–808.

Pongpiachan, S., 2015. A preliminary study of using polycyclic aromatic hydrocarbons as chemical tracers for traceability in soybean products. Food Control 47, 392–400.

Pongpiachan, S., Hattayanone, M., Pinyakong, O., Viyakarn, V., Chavanich, S., Bo, C., Khumsup, C., Kittikoon, I., Hirunyatrakul, P., 2017a. Quantitative ecological risk assessment of inhabitants exposed to polycyclic aromatic hydrocarbons in terrestrial soils of King George Island, Antarctica. Polar Science 11, 19–29.

Pongpiachan, S., Hattayanone, M., Suttinun, O., Khumsup, C., Kittikoon, I., Hirunyatrakul, P., Cao, J., 2017b. Assessing human exposure to PM10-bound polycyclic aromatic hydrocarbons during fireworks displays. Atmospheric pollution research 8 (5), 816–827.

Pongpiachan, S., Hattayanone, M., Tipmanee, D., Suttinun, O., Khumsup, C., Kittikoon, I., Hirunyatrakul, P., 2018. Chemical characterization of polycyclic aromatic hydrocarbons (PAHs) in 2013 Rayong oil spill-affected coastal areas of Thailand. Environ. Pollut. 233, 992–1002.

Sun, C., Zhang, J., Ma, Q., Zhang, F., Chen, Y., 2016. Risk assessment of polycyclic aromatic hydrocarbons (PAHs) in sediments from a mixed-use reservoir. Human and Ecological Risk Assessment: An International Journal 22 (2), 447–459.

Tamamura, S., Sato, T., Ota, Y., Wang, X., Tang, N., Hayakawa, K., 2007. Long-range transport of polycyclic aromatic hydrocarbons (PAHs) from the eastern Asian continent to Kanazawa, Japan with Asian dust. Atmos. Environ. 41 (12), 2580–2593.

US-EPA, 1989. Risk assessment guidance for superfund. In: Human Health Evaluation Manual. vol. 1 Washington D.C., USA. Retrieved from. https://www.epa.gov/sites/production/files/2015-09/documents/rags_a.pdf.

US-EPA, 1991. Risk assessment of guidance for superfund. *volume 1 - Human Health Evaluation Manual (Part b, Development of Risk-based Preliminary Goals)*. Washington DC, USA. Retrieved from. https://epa-prgs.ornl.gov/radionuclides/HHEMB.pdf.

US-EPA, 1993. Provisional Guidance for Quantitative Risk Assessment of Polycyclic Aromatic Hydrocarbons. US-EPA, Washington DC.

US-EPA, 2001. Risk assessment guidance for superfund. In: Part A, Process for Conducting Probabilistic Risk Assessment, vol. III. Office of Emergency and Remedial Response, Washington DC Retrieved from. https://www.epa.gov/sites/production/files/2015-09/documents/rags3adt_complete.pdf.

US-EPA, 2019. IRIS Database. Retrieved from. https://cfpub.epa.gov/ncea/iris/search/index.cfm.

Yang, X.Y., Okada, Y., Tang, N., Matsunaga, S., Tamura, K., Lin, J.M., Hayakawa, K., 2007. Long-range transport of polycyclic aromatic hydrocarbons from China to Japan. Atmos. Environ. 41 (13), 2710–2718.